Proceedings of CONF-MCEE 2027 Symposium: Advanced Nanomaterials and 2D Materials: Synthesis, Modeling, and Applications
DOI: 10.54254/2755-2721/2027.AD38964

Recycling and Reuse of Metal Powders in Electron Beam Powder Bed Fusion: A Review

Boxuan Wang

Xi'an Technological University Peter the Great St. Petersburg Polytechnic University Joint Polytechnic Institute, Xi'an Technological University, Xi'an, China
1768813360@qq.com

Abstract. Electron beam powder bed fusion (EB-PBF) is a vacuum-based metal additive manufacturing technique that selectively melts metal powder layers with a high-energy electron beam; it features low residual stress, high build efficiency and few support requirements, and is widely applied to near-net-shape fabrication of hard-to-machine alloys such as Ti-6Al-4V, Inconel 718 and γ-TiAl. After each build, approximately 95%–98% of the un-melted powder can be recovered, sieved and re-used, making powder recycling critical to both cost reduction and sustainable manufacturing. Focusing on literature of the past fifteen years (2011–2026) together with key earlier works, this review summarizes the recovery–reuse loop and powder characterization methods, and classifies powder degradation into chemical (oxidation and elemental evaporation at high temperature in vacuum), physical (mechanical damage, morphological deterioration and particle-size drift) and functional (loss of flowability and charging behavior) aspects. It then analyzes the effects of powder reuse on part density, microstructure, static strength, impact toughness and fatigue, fatigue performance being the most sensitive to powder state. Recycling behaviors of Ti-6Al-4V, Inconel 718, γ-TiAl, H13 steel, CoCrMo and copper powders are compared, followed by quality-control strategies such as fresh-powder blending, sieving management, in-process monitoring and standardization, and reported powder reuse limits. Remaining problems (scattered characterization approaches, lack of unified reuse criteria, insufficient in-situ monitoring) and future directions toward standardized powder-quality metrics, online monitoring and closed-loop recycling are discussed.

Keywords: electron beam powder bed fusion, metal powder recycling and re-use, powder degradation, oxygen content, fatigue performance

1. Introduction

Electron beam powder bed fusion (EB-PBF; commercially known as Electron Beam Melting) selectively melts metal powder layers with a high-energy electron beam in a vacuum chamber of about 10^{-4}–10^{-3} mbar [1, 2]. Compared with laser powder bed fusion (L-PBF), it offers higher energy density, faster build rates, lower residual stresses and better protection of reactive metals from oxidation [3, 4], and serves aerospace (Ti-6Al-4V structural parts, γ-TiAl turbine blades, Inconel 718 (IN718) components) and biomedical implants [5, 6]. A distinctive process feature is

© 2026 The Authors. This is an open access article distributed under the terms of the Creative Commons Attribution License 4.0 (https://creativecommons.org/licenses/by/4.0/).

DOI: 10.54254/2755-2721/2027.AD38964

powder-bed preheating: to prevent "smoking", the ejection of charged particles from the bed by Coulombic repulsion, the bed must be preheated to a semi-sintering temperature so that conductive networks form between particles [7, 8]; the preheating temperature differs markedly between alloys, about 1,000 °C for IN718 and about 650 °C for Ti-6Al-4V [9]. Preheating sinters the powder around the parts into a cake, which must be blasted off with a powder recovery system (PRS) and sieved before reuse [4, 10]. Recovery is thus built into the process itself: after each build, 95%–98% of the un-melted powder can be recovered and recycled, and since powder feedstock accounts for about 28% of the cost of a single build, recovery is a precondition of commercial viability — decisive for expensive pre-alloyed powders such as γ-TiAl [1, 11]. At the same time, repeated recovery changes the composition, morphology, particle size distribution (PSD) and rheology of the powder, and hence part properties, making recycling a reliability-driven engineering problem [6, 12].

Research has focused on five issues: characterization and mechanisms of powder degradation; effects of recovery on part microstructure and mechanical properties (especially fatigue); differences between material systems; quality-control strategies such as replenishment, sieving management, monitoring and standardization; and the definition of reuse limits. Systematic work has also been carried out in China: Tang reviewed more than a decade of engineering practice with powder bed electron beam additive manufacturing of Ti-6Al-4V [13]; Liu et al. reviewed the defects, microstructure and mechanical properties of electron-beam-built Ti-6Al-4V [14]; Zhang et al. and Hu et al. reviewed powder reuse mechanisms and recovery processes [15, 16]; Pan et al. summarized the cyclic reuse of metal powders and proposed three replenishment strategies [17]; Chen et al. proposed "circular additive manufacturing", extending recycling to scrap metal [18]; and Jiao et al. comprehensively reviewed EB-PBF and its development in China [19]. These reviews either cover all powder bed fusion/AM processes or are limited to a single alloy and a single stage; none has systematically focused on powder recovery and reuse in EB-PBF across material systems.

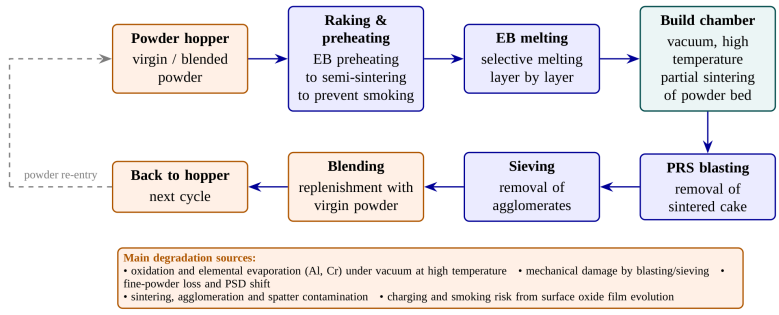


Figure 1. Schematic of the closed-loop recovery and recycling flow of EB-PBF metal powders and the main powder degradation sources (dashed arrow: re-entry of the recycled powder into the hopper)

The field has developed through three stages: pioneering powder-fraction comparisons and the process-level foundation [20, 21]; the 2015–2019 stage, in which Tang et al. and Petrović et al. established the Ti-6Al-4V paradigm with oxygen content as the primary indicator [22, 23]; and a systematic stage since 2020 covering reuse limits, fatigue, biomedical applications, online monitoring and degradation frameworks, complemented by broader powder-bed-fusion and whole-workflow reviews [1, 24-28]. The focus is shifting from whether the powder can be reused to how to reuse it scientifically [6, 12]. Taking the unique features of EB-PBF — vacuum preheating, smoking prevention, PRS recovery and the distinctive behavior of TiAl and pure copper — as the main thread, this review synthesizes this literature, with special attention to representative Chinese

DOI: 10.54254/2755-2721/2027.AD38964

production-scale work. The closed-loop recovery and recycling flow is illustrated in Figure 1; Section 2 introduces the process, powder requirements and characterization; Section 3 reviews degradation mechanisms; Section 4 analyzes effects on part quality; Section 5 compares material systems; Section 6 summarizes recycling strategies, quality control and standards; Section 7 discusses remaining problems and outlook; Section 8 concludes.

2. EB-PBF process, powder characteristics and recycling flow

2.1. Powder requirements

Metal powders for EB-PBF are typically produced by plasma atomization, gas atomization or plasma rotating electrode processing, with a nominal particle size range of 40–105 μm, and powder can be recycled to a large extent [21]. Because the powder bed must dissipate electron-beam charging through inter-particle conductivity, the powder needs good sphericity, a clean surface and a controlled PSD: irregular particles lower the packing density of the raked layer and make parts swell and overheat, while coarse particles cause in-situ segregation and raking streaks [1, 2].

2.2. The powder recovery and recycling loop

After building, the sintered cake is blasted off with the PRS; the recovered powder is sieved (removing agglomerates, inclusions and over-sintered particles), mixed with the hopper powder, optionally replenished with fresh powder and returned to the next cycle [4, 5, 23]. The preheating after raking is the key element for understanding degradation: build temperatures range from about 300 to 1,100 °C and the electron beam repeatedly scans the layer at about 10 m/s, so the repeated high-temperature exposure defines the cumulative thermal history of the powder and controls its degradation rate [7, 21]. In industrial practice, because EB-PBF hoppers hold about 100–180 kg of powder, the recovered powder of a single cycle often cannot fill the hopper independently; blending recycled powders of different generations and with virgin powder is therefore the norm, making the reuse effect hard to isolate and contributing to the divergent early conclusions [1].

2.3. Powder characterization methods

Powder degradation research relies on a combination of characterization techniques: SEM and dynamic image analysis for morphology and particle size; the FT4 rheometer and rotating drum (GranuDrum) for basic flow energy (BFE), specific energy (SE), angle of repose (AOR) and cohesion index (CI); tap density for the Hausner ratio (Hr) and Carr index (C); inert-gas fusion (LECO) for oxygen and nitrogen; X-ray photoelectron spectroscopy (XPS) and Auger electron spectroscopy (AES) for the surface oxide film thickness and chemical states [1, 8, 29, 30]. Bulk oxygen by inert-gas fusion is the most widely reported degradation indicator, integrating oxidation, evaporation and replenishment dilution into one number tied to the oxygen limit of ASTM F2924 [31]; flowability, in contrast, is instrument-dependent — rankings can even reverse between instruments — and must be interpreted together with morphology and chemistry data [1].

3. Degradation mechanisms of powders during recovery and reuse

Recovered EB-PBF powder degrades along three coupled levels: chemical degradation dominated by oxygen/nitrogen pickup and elemental evaporation; physical degradation manifested as morphological damage, PSD drift and agglomeration; and functional degradation reflected in

DOI: 10.54254/2755-2721/2027.AD38964

flowability, spreadability and charging behavior. Together they determine how many times a powder can be reused.

3.1. Chemical degradation: oxygen/nitrogen pickup and elemental evaporation

Oxygen pickup is the most closely monitored degradation indicator for Ti-6Al-4V powder, the upper limit being 0.20 wt.% per ASTM F2924 [31]; representative evolutions are shown in Figure 2. Reported rates and starting contents differ markedly: Tang et al. measured 0.08→0.19 wt.% over 21 reuse cycles and attributed the pickup mainly to air exposure during recovery blasting and sieving [22]; based on the same production tracking over hundreds of builds, the group of Tang Huiping set cyclic use limits of 4 and 21 cycles for Ti-6Al-4V ELI and Ti-6Al-4V powders, respectively [13]; Sun et al. measured 0.15→0.205 wt.% after 30 cycles (about 37%, slightly exceeding the limit) [10]; Petrović and Niñerola tracked recovered powder under the worst case without replenishment and found the content, initially 0.14 wt.%, crossing the limit after about 12 cycles, attributing the pickup to moisture released from the chamber walls [23]; Nandwana et al. measured 0.13→0.18 wt.% within 5 cycles with nitrogen essentially unchanged [32]; Ghods et al. found the oxygen content exceeding 0.20 wt.% after only 11 cycles [33]; Shanbhag and Vlasea measured a 37% increase within 3 cycles (the third-generation powder G3 still below 0.18 wt.%) and extrapolated from the logarithmic trend a reuse life of about 5–6 cycles [1]; and Popov et al. measured 0.124→0.324 wt.% under extreme conditions (69 reuse cycles) [3]. The number of cycles sustainable thus depends strongly on the starting oxygen content and the replenishment strategy — the lower the starting content and the more complete the replenishment, the more cycles can be sustained (Figure 2).

Regarding where the oxygen goes, Sun et al. found that after 30 cycles the surface oxide film thickness was essentially the same as that of virgin powder, the excess oxygen being mainly dissolved in the β phase, and that highly oxidized particles were distributed highly inhomogeneously within the recovered batch [10]. Soundarapandiyan et al. distinguished powder types: the pickup amounted to about 0.03 wt.% per build in sintered cake but only 0.003–0.004 wt.% per build in mixed recovered powder [4]. Sources include the reaction of residual moisture and oxygen in the chamber with titanium at high temperature, moisture adsorbed during ambient exposure, and the fresh oxide surfaces created by blasting and sieving [1]. Oxygen dissolves interstitially in the α phase, increasing strength but decreasing ductility, and may promote pore formation in the melt pool [1, 6]. Oxidation in EB-PBF is often faster than in L-PBF owing to the high preheating temperature, and adding low-oxygen fresh powder (e.g. ELI grade) is an effective control strategy [34]. Nitrogen rises much more slowly: Shanbhag and Vlasea measured a 44% increase within 3 cycles (0.016→0.023 wt.%), still far below the 0.05 wt.% limit of ASTM F2924 and following a logarithmic saturation trend characteristic of surface contamination [1].

The surface oxide film evolves continuously during reuse (Figure 3). Cao et al. quantified the film of Ti-6Al-4V powder by XPS/AES: the average thickness increased from about 6.5 nm (virgin) to 7.35 nm after 5 cycles and 7.54 nm after 10 cycles, the reused film being thicker but more uneven; the surface Al content dropped from 27.6 at.% (well above the nominal value, owing to preferential oxidation of Al) to 14.6 at.% after 5 cycles and 15.9 at.% after 10 cycles, reflecting two competing processes, evaporation of Al and its preferential oxidation under vacuum at high temperature [29]. For IN718, Gruber et al. found that the uniform thin oxide film of virgin powder transformed after the first build into a non-uniform film rich in stable Al-oxide particles (50–200 nm), with oxygen rising from 146 ppm (virgin) to 215 ppm after the first cycle and 266 ppm after 14 cycles (about 500 cumulative hours) [30]; Cordova et al. measured an oxygen increase of about

DOI: 10.54254/2755-2721/2027.AD38964

20%, surface Al-rich oxide particles of 100–200 nm and an average film thickness of about 13 nm [8].

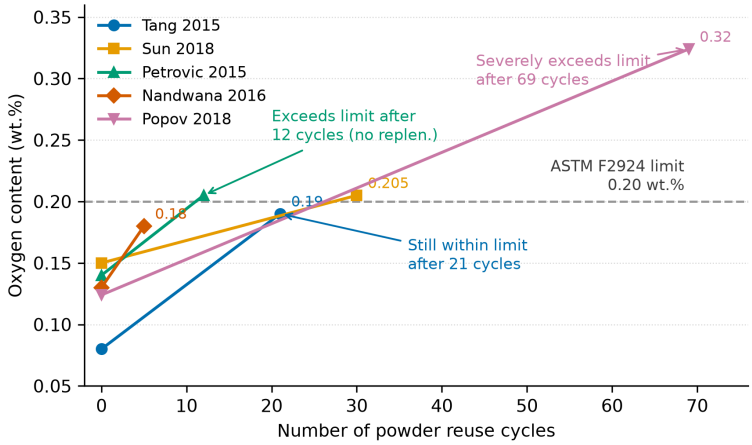


Figure 2. Evolution of the oxygen content of Ti-6Al-4V powder with reuse cycles (data from Tang 2015 [22], Sun 2018 [10], Petrović 2015 [23], Nandwana 2016 [32] and Popov 2018 [3]; dashed line: the 0.20 wt.% oxygen limit of ASTM F2924 [31])

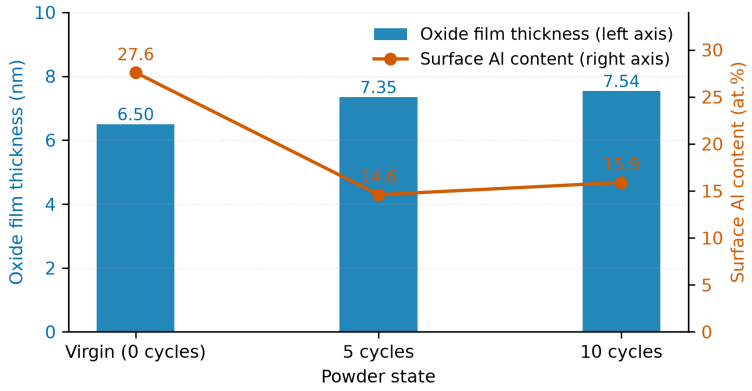


Figure 3. Changes of the surface oxide film thickness and the surface Al content of Ti-6Al-4V powder with reuse cycles (XPS/AES data from Cao et al. [29])

Elemental evaporation acts in the opposite direction. In Ti-6Al-4V, Al evaporates preferentially from powder surfaces and melt pools [23, 29]; Tang et al. measured a decrease of Al in built parts from 6.35 to 5.93 wt.% after 21 reuse cycles [22]. For γ-TiAl the loss is particularly critical: Schwerdtfeger and Körner showed Al losses of several atomic percent when building Ti-48Al-2Nb-2Cr [35], and Wang et al. measured in a 70-cycle study of Ti-48Al-2Cr-2Nb a continuous decrease of Al from 48.43 to 46.31 at.% [11]. For IN718, Raza and Hryha demonstrated with heat-shield deposits that Cr is the dominant evaporating element — the condensate consists mainly of Cr oxide, and although the equilibrium vapor pressure of Cr is second only to that of Al, its content is about 40 times higher; evaporation may also weaken the corrosion resistance and high-temperature performance of built parts [9]. The compositional evolution of IN718 and TiAl powders is summarized in Figure 4.

DOI: 10.54254/2755-2721/2027.AD38964

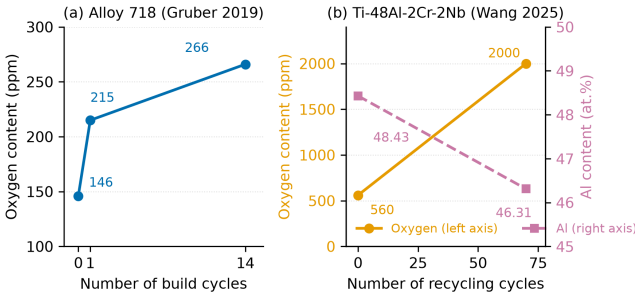


Figure 4. Compositional evolution of IN718 and TiAl powders: (a) oxygen content of IN718 powder vs. build cycles (data from Gruber et al. [30]); (b) oxygen content (left axis) and Al content (right axis) of Ti-48Al-2Cr-2Nb powder vs. recycling cycles (data from Wang et al. [11])

Siblani et al. established a high-temperature oxidation kinetics model for spherical Ti-6Al-4V powder predicting oxygen pickup under different temperature–time conditions [36], and Hryha proposed a general degradation framework covering the full powder life cycle, with degradation rates depending strongly on alloy composition and processing technology [25].

3.2. Physical degradation: morphology, particle size and agglomeration

Karlsson et al. compared parts built from 25–45 μm and 45–100 μm Ti-6Al-4V fractions and found that particle size and layer thickness had no significant effect on bulk microstructure and mechanical properties, whereas the surface morphology differed markedly — particle size affects part quality mainly through the surface state [20]. Repeated reuse deteriorates particle morphology: SEM observations show surface defects such as deformation, fracturing, clipping/clap, impact marks, spatter particles and agglomerates, where fracturing and deformation arise mainly from the mechanical action of PRS blasting and sieving and the spatter and agglomerates from overheating and sintering [1, 33]; compared with virgin powder, recovered powder has fewer satellites, rougher surfaces and lower sphericity [37].

Reuse also shifts the PSD: fine powder is lost and D10, D50 and D90 increase overall — Shanbhag and Vlasea reported increases of 7%, 10% and 7% for G3 powder (Figure 5), and Ghods et al. observed PSD narrowing, particle fracturing and decreased sphericity within 30 cycles [1, 33]. Industrial batch studies by the Pangang team in China showed that after cyclic use the fine fraction decreases and inter-particle bonding increases, with D10, D50 and D90 increasing from about 33.6, 59.4 and 89.6 μm to about 45.9, 74.8 and 111.6 μm (Figure 6a in Section 5.1), while blocky residues from heat-shield deposits and PRS cleaning debris gradually accumulate [38]. Spatter is another contamination source: spatter collected on the IN718 heat shield reached 2,540 ppm oxygen, about 17 times that of virgin powder (<150 ppm); covered by oxidized condensate it adheres firmly to the shield and rarely contaminates the bed, but the risk remains when the shield is poorly maintained [9].

3.3. Functional degradation: flowability, packing and charging behavior

Changes of flowability with reuse are highly method-dependent and among the most inconsistent conclusions in the literature. For G3 powder, the FT4 rheometer measured +18% basic flow energy and +15% specific energy vs. virgin, and the Hausner ratio and Carr index also rose (by 3% and 30%); conversely, the angle of repose and cohesion index measured by the rotating drum decreased

DOI: 10.54254/2755-2721/2027.AD38964

with reuse, attributed to larger particles and fewer fines — based on the constant-cohesion-index range (drum speeds of 15–40 rpm, corresponding to raking speeds of 75–175 mm/s), the authors recommended this raking speed range (Figure 5) [1]. The direction of change is not consistent between studies: Tang et al. observed improved flowability after reuse, attributed to a narrower PSD and fewer satellites [22]. Powder usability should therefore be evaluated in the way closest to the actual raking process [1].

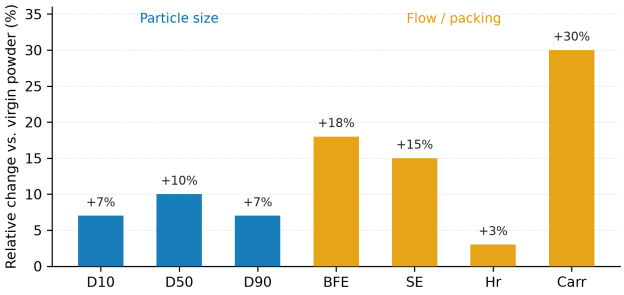


Figure 5. Relative changes of the particle size and flow/packing metrics of G3 (third-generation recycled) powder vs. virgin powder (data from Shanbhag and Vlasea [1])

The electrostatic charging behavior is particularly important for process stability. Cordova et al. measured a significantly enhanced charging ability of reused IN718 powder (charge per unit mass from −5.84 to −9.18 V/g, about 1.6 times), attributed to the surface oxide film acting as an insulating medium; this increases the risk of smoking [8]. Chiba et al. explained smoking mechanistically: nanometer-thick transition-metal oxides (e.g. Cr_2O_3, TiO_2) on particle surfaces are Mott insulators hindering inter-particle conduction, so charge accumulates until Coulombic repulsion ejects the particles; preheating suppresses smoking by lowering the film resistance, and mechanical stimulation can induce an insulator–metal transition — pointing to mechanical pretreatment as a viable regeneration route [7].

4. Effects of powder recovery on part quality and performance

The effects of powder degradation on part quality follow three main paths: oxygen pickup raises strength through interstitial solid-solution strengthening while reducing ductility; fine-powder loss and morphological deterioration induce lack-of-fusion defects that mainly impair fatigue; and post-treatments such as hot isostatic pressing (HIP) can partially mitigate these effects.

4.1. Density and defects

Ghods et al. observed no significant change in part porosity within 30 reuse cycles and concluded that internal porosity in EB-PBF is controlled mainly by process parameters rather than by powder state [39]; Chandroth et al. likewise observed, within 5 reuse cycles, conventional defects (pores and lack-of-fusion) in the 2–80 μm range with porosity increasing with build height, and only a slight porosity increase from recovered powder in regions far from the base plate [37]. Soundarapandiyan et al., however, pointed out that reuse reduces fine powder and increases high-aspect-ratio particles, which may create voids in the raked layer and induce lack-of-fusion defects, degrading high-cycle fatigue performance [4]. For IN718, Gruber et al. found a clear positive correlation between powder oxygen content and the number of oxide inclusions in parts: the defects comprise dispersed oxide particles within lack-of-fusion regions and large Al-rich agglomerates in the matrix, originating from

DOI: 10.54254/2755-2721/2027.AD38964

the Al-rich oxides on the surface of reused powder; even after HIP they remained difficult to eliminate [40].

4.2. Microstructure

Compositional changes propagate into the microstructure. Ghods et al. observed that with increasing reuse cycles the parts developed a finer basketweave with an increasing α surface/volume ratio, and the α laths thickened slightly (from about 1.0 to 1.4 μm), while the α volume fraction showed no clear trend [33, 41]. EBSD studies by Popov et al. showed that specimens from severely reused (69-cycle) powder had slightly smaller α grain sizes (1.5 μm vs. 1.8 μm) and a lower β phase fraction (1.7% vs. 3.3%); phase transformation still followed the Burgers orientation relationship, texture showed an inheritance effect through repeated thermal cycling, and anisotropy was not significant [5]. In contrast, Chandroth et al. found in a biomedical implant study that although virgin and recovered powder differed in morphology and surface composition, the implant microstructures differed very little — acicular martensite with colony and basketweave α/β following the Burgers orientation relationship, essentially the same evolution with build height for both powders, and only a slight porosity increase in lattice regions far from the base plate [37]. The microstructural effects of powder degradation are thus partly blunted.

4.3. Static mechanical properties

The interstitial solid solution of oxygen slightly increases the strength of parts built from reused powder. Popov et al. reported higher strength and lower elongation for specimens from 69-cycle powder [3]; Soundarapandiyan et al. found that within 10 cycles the yield and ultimate tensile strengths increased slightly while elongation, hardness and Charpy impact energy were almost unaffected [4]; Schur et al. observed strength increase accompanied by a marked decrease in ductility [42]; and Wanjara et al. confirmed under industrial conditions with 3D part nesting and powder reuse that when oxygen exceeded 0.20 wt.% the ductility was impaired, and that surface state and oxygen content significantly affected fatigue performance [43]. Grell et al. showed that increasing oxygen content significantly reduces the impact toughness of EB-PBF Ti-6Al-4V [44]. Schur et al. further showed that reuse markedly intensifies mechanical anisotropy: the horizontal elongation decreased by more than 60% within 30 builds (about 1.5 times the vertical decrease), related to the microstructural evolution caused by the increasing oxygen content [42]. As for hardness, some studies reported higher hardness owing to oxygen pickup and grain refinement [5, 45], while others found hardness almost unaffected [4]. The life-cycle review of Ren et al. further showed that aluminum alloys are the most sensitive to powder state (largest losses, especially elongation), whereas titanium alloys, steels and Ni-based superalloys may gain strength but usually lose elongation — reuse limits must weigh strength and ductility simultaneously [26].

4.4. Fatigue performance

Fatigue is widely regarded as the mechanical indicator most sensitive to powder state [12]. Soundarapandiyan et al. showed that reuse increases lack-of-fusion defects and markedly degrades high-cycle fatigue performance [4]. Fractographic analysis by Schur et al. showed that the rough as-built surface acts as a stress raiser whose influence on fatigue life can even exceed that of powder degradation itself; after machining off the surface layer (roughness reduced from about 30 μm to about 1.7 μm), crack initiation shifted from the surface to the interior and the consistency of fatigue

DOI: 10.54254/2755-2721/2027.AD38964

performance improved markedly [46]. Borrelli et al. showed that reuse reduces satellites and pores, induces grain coarsening and increases oxygen content and hardness; the critical defect size increased with reuse, but no significant difference in fatigue behavior was found [45]. Bellini et al. compared virgin, 5-cycle and >100-cycle powder specimens and found no significant effect of reuse on crack growth rates — internal defects dominate crack growth and mask the powder state [47]. For biomedical implants, Chandroth et al. noted that the fatigue life of parts from reused powder (about 10^4–10^6 cycles) fell below the implant design standard requirement (about 10^5–10^7 cycles), mainly attributed to thickening of the surface oxide film and a higher defect fraction, while HIP can largely restore fatigue performance [37]. Overall, the effect of powder reuse on fatigue is mediated indirectly through powder changes that induce lack-of-fusion defects and through the surface state, rather than through the oxygen content itself [12].

4.5. The role of post-processing

Hot isostatic pressing is an effective means to mitigate the negative effects of powder reuse. Popov et al. confirmed that HIP significantly restores the fatigue resistance of specimens from severely reused powder, so that such powder can still serve non-critical load-bearing applications; HIP simultaneously coarsens the α grains (to about 2.5–2.7 μm) and increases the β phase fraction, partially homogenizing the reuse effects [3, 5]. For IN718, however, although HIP achieves near-full densification, the Al-rich oxide inclusions in parts built from recovered powder largely persist [40].

5. Recycling and reuse behavior of different material systems

The dominant degradation mechanism differs between alloys, which determines their respective reuse strategies and limits; Table 1 summarizes the research status of the main material systems.

Table 1. Comparison of powder recovery and reuse behavior of the main EB-PBF material systems

Material system	Dominant degradation mechanism	Reported reusability	Key findings and strategies
Ti-6Al-4V	oxygen pickup and Al evaporation; mechanical damage during recovery	virgin O about 0.08–0.15 wt.%; typical limit 0.20 wt.%; about 5–12 cycles to reach the limit (replenishment-dependent) [1, 10, 22, 23, 33]	slight strength increase; ductility and fatigue sensitive; blending and HIP effectively extend reuse [4, 5]
Inconel 718 (IN718)	formation of surface Al-rich oxide particles; Cr evaporation; charging / smoking risk	O 146→266 ppm (14 cycles); chemical composition relatively stable; reuse limited by physical properties [30, 32]	oxide inclusions grow with oxygen and are hard to remove by HIP; charging ability of reused powder increases by about 1.6 times [8, 40]
γ-TiAl	severe Al evaporation; phase transformation ($\alpha/\alpha_2 \rightarrow \gamma$+B2); Laves phase precipitation	O 560→2000 ppm, Al 48.4→46.3 at.% (70 cycles) [11]	reuse markedly reduces ductility; maintaining a 15%–30% fresh-powder fraction gives the best cost–performance [11, 48]
H13 tool steel	morphological deterioration; O/N pickup	O 149→250 ppm, N 237→394 ppm (16 cycles) [49]	larger particle size improves powder bed packing; hardness of parts unaffected [49]
CoCrMo (medical)	— (EBMR remelting of scrap)	remelting removes volatile impurities such as Fe, Mn and Si and enriches Co; W and Nb are hard to remove [50]	hardness 520–600 HV controllable; tends to converge after heat treatment [51]
Pure copper	oxygen content strongly affects process and properties	oxygen accumulation mechanism clarified [52, 53]	high-oxygen powder requires an adjusted process window [53]

DOI: 10.54254/2755-2721/2027.AD38964

5.1. Ti-6Al-4V

Ti-6Al-4V is the most thoroughly studied material in EB-PBF, with the largest number of powder reuse studies and the most complete datasets; its degradation is dominated by oxygen pickup (Figure 2) [1, 4, 10, 22, 23, 33, 45]. Solid-solution strengthening by oxygen increases strength and hardness but impairs ductility and impact toughness; fatigue is sensitive to powder state but mediated mainly through defects. In industry, reuse is managed through the combined use of replenishment, sieving and HIP; reported reuse limits range from about 5–12 cycles without replenishment to tens of cycles with replenishment (Figure 8).

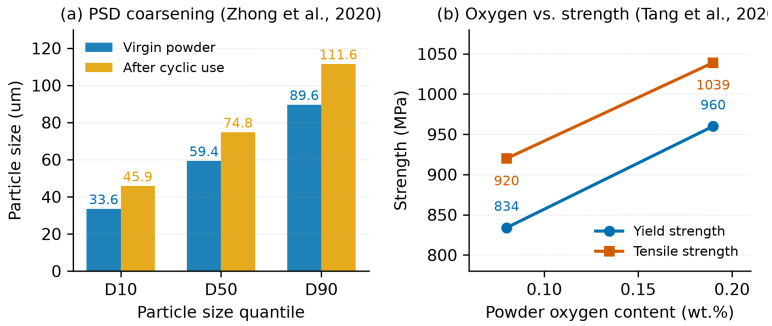


Figure 6. Supplementary data from Chinese studies: (a) coarsening of the particle size distribution of Ti-6Al-4V powder before and after cyclic use (data from Zhong et al. [38]); (b) effect of the powder oxygen content on the yield and ultimate tensile strengths of parts (data from Tang Huiping et al. [13], based on production tracking over hundreds of builds, corresponding to 0 and 21 cycles)

Chinese industrial practice likewise supports this paradigm. Zhong et al. reported that after 10 cycles of use the old powder showed preheating smoke, powder spattering and poor melting, and the relative density of parts decreased from about 95% to about 92%; replenishing fresh powder at a volume ratio of about 3:1 slowed the deterioration of powder properties [38]. As described in Section 3.1, the group of Tang Huiping set cyclic use limits of 4 cycles for ELI and 21 cycles for TC4, and observed that as the powder oxygen content increased from 0.080 to 0.190 wt.%, the yield and ultimate tensile strengths of parts increased from 834 and 920 MPa to 960 and 1,039 MPa (Figure 6b) [13]. These values are consistent with Tang et al. [22] (the same production tracking; Figure 2), confirming the oxygen-based reuse paradigm in Chinese industrial applications.

5.2. Inconel 718

Unlike Ti-6Al-4V, the composition of IN718 stays relatively stable over many cycles; its reuse limit is determined mainly by physical properties such as flowability rather than by oxygen content [32]. Figure 4a shows that the oxygen content of IN718 powder rises slowly with build cycles (146→215→266 ppm), far below the Ti-6Al-4V limit system in absolute terms [30]. Reuse forms Al-rich oxide particles on the powder surface; once these enter the parts they are hard to eliminate by HIP and are a key factor affecting part quality [30, 40]. Cr evaporation and the insulating surface oxide film strengthen the charging ability of reused powder, increasing the smoking risk [7-9].

DOI: 10.54254/2755-2721/2027.AD38964

5.3. γ-TiAl

γ-TiAl depends particularly on powder recycling because the powder is expensive and hard to machine. The systematic study of Ti-48Al-2Cr-2Nb by Wang et al. revealed its distinctive degradation mechanism (Figure 4b): besides oxygen pickup (560→2,000 ppm, at 22–28 ppm per cycle), the continuous Al loss (48.43→46.31 at.%) and the phase transformations induced by prolonged exposure at 900–1,150 °C (α/α_2→γ+B2 and C14 Laves phase precipitation after 30 cycles) are the more prominent degradation features, and the surface oxide film changes from a TiO_2/Al_2O_3 mixture (54:46) to an Al_2O_3-dominated composition (82%) [11]. Degradation reduces part ductility by about 40%; maintaining a 15%–30% fresh-powder fraction optimizes the cost–performance balance [11]; the underlying reusability mechanisms were further clarified by Wang et al.) [48].

5.4. Other materials

Yang et al. characterized the reuse behavior of H13 tool steel powder over 16 build cycles: oxygen increased from 149 to 250 ppm and nitrogen from 237 to 394 ppm; larger and more irregular particles lowered flowability, but the relative packing density of the powder bed improved because of the broadened PSD, and part hardness was not significantly affected [49]. For CoCrMo, Vutova et al. explored direct recycling of medical CoCrMo scrap by electron beam melting refining (EBMR): at about 1,860 K and a 20-min hold, volatile impurities such as Fe, Mn and Si are efficiently removed (Fe about 81.5%, Si about 65.1%, Mn completely at lower temperatures) with Co enrichment, while W and Nb, having low vapor pressures, can hardly be removed (about 3% and 6%, with W still exceeding the ASTM F75 limit); the ingots show pronounced microsegregation [50]. Their follow-up metallographic study showed that heat treatment markedly changes the ingot microstructure: as the refining temperature increases, grains after heat treatment grow from about 50 μm to about 200 μm with markedly fewer interdendritic precipitates, and the hardness of the recycled alloy (520–600 HV) can be further tuned through process parameters and heat treatment [51].

Because oxygen strongly affects melt pool behavior and electrical conductivity in pure copper, Guschlbauer et al. and Gu et al. studied copper powder reuse from the perspectives of the process window and the oxygen accumulation mechanism; TEM characterization by Gu et al. revealed that oxygen mainly precipitates as ultra-fine round oxide particles of about 50 nm in the copper matrix [52, 53]. Blasco Puchades et al. compared two copper powder management strategies (Figure 7): in the batch-recovery SINT method, the oxygen content accumulated linearly at about 23.7 ppm per cycle (from about 15–30 ppm at SN0 to 165 ppm at SN6 and 236 ppm at SN8; SN7/SN8 were excluded from the trend fit because the preheating temperature had to be raised to suppress smoking, and by SN9 stable building was no longer possible), while the relative density of parts decreased from 98.88% at SN0 to 96.81% at SN6; in the continuous-replenishment THIRD method (fresh powder replenishment with strict humidity control), the oxygen content never exceeded 170 ppm within 59 cycles, with part relative density above 99.38% and electrical conductivity above 99.5% IACS — the replenishment strategy is critical for long-term reuse of pure copper [54].

DOI: 10.54254/2755-2721/2027.AD38964

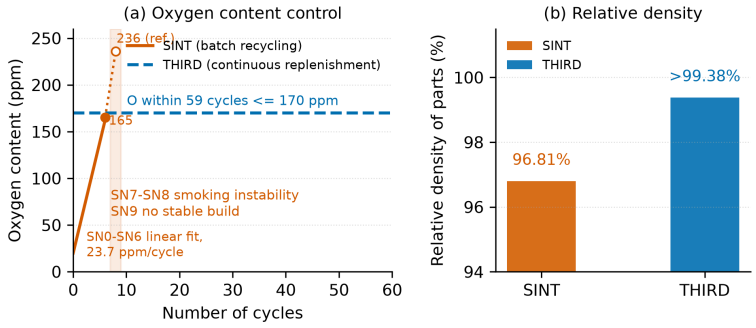


Figure 7. Comparison of two powder management strategies for pure copper (data from Blasco Puchades et al. [54]): (a) oxygen accumulation in the batch-recovery SINT method vs. the continuous-replenishment THIRD method; (b) part relative density under the two strategies

6. Recycling strategies, quality control and standards

6.1. Fresh-powder replenishment and blending strategies

Blending in fresh powder is the most direct means to extend powder life and stabilize powder quality. Shanbhag and Vlasea blended recycled powders of different generations pairwise in equal mass ratios ; blend properties lay essentially between those of the constituents [1]. For TiAl, Wang et al. recommended a 15%–30% fresh-powder fraction (Section 5.3) [11]; for Ti-6Al-4V, Petrović et al. made clear that their 12-cycle limit represents the worst case without replenishment and that adding fresh powder markedly improves reusability [23]. Blending also brings new problems: locally inhomogeneous mixing of powders with different oxygen contents may cause oxygen and strength fluctuations within a single build, requiring homogenization and batch traceability management [1]. Chinese reviews agree: Zhang et al. classified reuse methods into single-batch cyclic use and virgin-powder replenishment, and normalized the recovery flow into cooling and collection, crushing and sieving under inert atmosphere, and vacuum-sealed labeled storage, all under inert atmosphere with dry storage [15]; Hu et al. analyzed seven categories of factors affecting reuse (powder characteristics, production method, recovery source and handling, equipment, part geometry, process, and reuse strategy), noting that overflow powder differs little from virgin powder, while fresh-powder blending extends reuse cycles but reduces batch traceability [16]. The weight of each factor differs between material systems, so a generic list cannot be translated directly into quantitative strategies for each alloy.

Pan et al. classified the powder cycling strategies of powder bed fusion into three types: full recycling (no fresh powder; simple but with accumulating degradation), quantitative replenishment (fresh powder added after each build to keep the total constant, effectively diluting aged powder) and periodic replenishment (no replenishment for the first N builds followed by one full replenishment, balancing cost and performance); in critical applications with strict powder quality and traceability requirements, such as aerospace and biomedicine, controlled quantitative replenishment is currently preferred [17]. For quantitative execution, Hu et al. proposed a quality-control method built on the cycle coefficient, achieving linearly predictable management of cyclic TC4 powder use in laser powder bed fusion — a framework transferable to replenishment and blending management in EB-PBF [55].

DOI: 10.54254/2755-2721/2027.AD38964

6.2. Sieving and particle size management

Sieving is a key quality-control node: it removes agglomerates and coarse irregular particles and narrows the PSD, but a mesh too fine loses functional fines, one too coarse may retain harmful particles, and the mesh must match the target layer thickness [1]. Using a rotating-drum-type powder rheometer, Cordova et al. measured an avalanche angle of reused IN718 powder that decreased from 37° to 30°, indicating improved flowability with reuse; the upper rotation-speed limit of the instrument (corresponding to a recoater speed of about 250 mm/s) provides methodological grounds for correlating rheological characterization with actual raking conditions [8].

6.3. Process monitoring and data-driven management

Assessing powder state from the process logs and monitoring images inherent to EB-PBF is a recent trend; monitoring is evolving from offline sampling to online/in-situ approaches. Chandrasekar et al., based on statistical analysis of Arcam process log data, found that IN718 powder required more raking operations with increasing reuse cycles — spreadability degrades with reuse, and process logs can serve as an indirect powder quality indicator [56]. Gardfjell et al. developed in-situ electron optical imaging (ELO), which distinguishes single foreign particles of about 100 μm by backscattered-electron contrast — the signal intensity correlating with the effective atomic number of the alloy — enabling online detection of powder bed inclusions; a single tantalum particle in TNM powder, for example, appears clearly brighter (about 27 wt.% Ta by EDXS) [24].

6.4. Standards and reuse limits

ASTM F2924 specifies upper limits of 0.20 wt.% for oxygen and 0.05 wt.% for nitrogen in Ti-6Al-4V powder, the most commonly used criteria for judging whether the powder can continue to be reused [1, 31]; ASTM F3049 guides the characterization of metal powders for additive manufacturing, covering virgin and recycled powders [57]; and ASTM F3302 specifies the performance requirements of titanium alloy parts fabricated by powder bed fusion, forming with F2924 a quality standard system spanning powder and parts [58]. In China, GB/T 34508-2017 specifies the requirements, test methods and inspection rules of TC4 dense material for powder bed electron beam additive manufacturing [13, 59], and GB/T 44194-2024 specifies the general requirements, strategies, testing and process control for metal powder reuse in additive manufacturing — the special national standard directly governing the reuse flow [17, 60].

Reported reuse limits differ widely; Figure 8 summarizes the main results: from about 5–6 cycles (logarithmic extrapolation without replenishment) [1], 11 cycles [33] and 12 cycles [23] to 21 cycles [22], 30 cycles [10] and even 69 cycles (with HIP remediation) [5]; the results judged by the oxygen limit (mainly about 5–12 cycles) are generally lower than those judged by acceptable static performance (21 cycles reported by Tang et al.), and Sun et al. regarded 30 cycles — at which the oxygen content had reached 0.205 wt.%, slightly above the limit — as the reuse upper limit in most cases. Table 2 summarizes the experimental designs and core data of representative Ti-6Al-4V reuse studies (ESF is the EB-PBF suitability factor proposed by Shanbhag and Vlasea, a composite powder quality index defined in Section 7). The maximum number of reuse cycles is not a material constant but an engineering decision variable jointly determined by the recovery flow, the replenishment strategy, the oxygen limit requirement and the application grade of the parts [6, 12].

DOI: 10.54254/2755-2721/2027.AD38964

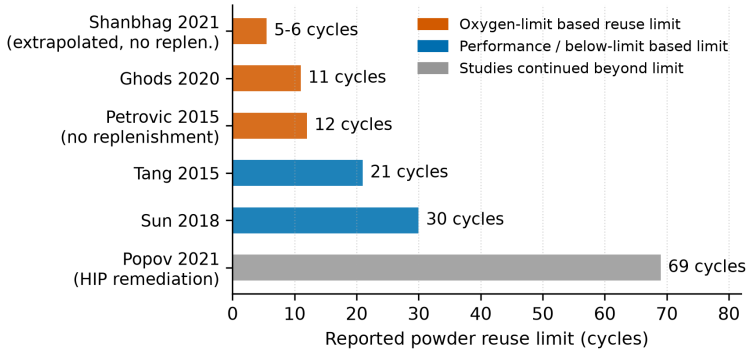


Figure 8. Comparison of reported Ti-6Al-4V powder reuse limits (red: judged by the ASTM F2924 oxygen limit; blue: judged by acceptable static performance or below-limit observation; grey: studies continued beyond the limit; data sources: [1, 5, 10, 22, 23, 33])

Table 2. Summary of data from representative Ti-6Al-4V powder reuse studies

Study	Reuse cycles	Oxygen content change (wt.%)	Other key metrics	Core conclusion
Tang 2015 [22]	21	0.08→0.19	Al slightly down (6.35→5.93)	static tensile properties consistent within 21 cycles
Petrović 2015 [23]	12	0.14→ above 0.20 (about 12 cycles)	no replenishment (worst case)	oxygen exceeds limit after 12 cycles; replenishment required
Nandwana 2016 [32]	5	0.13→0.18	nitrogen unchanged	oxygen pickup is the dominant degradation indicator
Sun 2018 [10]	30	0.15→0.205 (slightly above 0.20)	surface oxide film thickness essentially unchanged; excess oxygen dissolved in β phase	oxygen slightly above the limit at 30 cycles; regarded as the reuse upper limit in most cases
Popov 2018 [3, 5]	69	0.124→0.324	HIP restores fatigue performance	usable beyond the limit with HIP
Ghods 2020 [33]	30 (over limit at 11)	above 0.20	refined structure, thicker α laths, narrower PSD	no trend in α volume fraction
Shanbhag 2021 [1]	3 (extrapolated 5–6)	+37% (G3 still <0.18)	N +44%; flow metrics diverge	ESF composite index increases from 0.176 to 0.659
Soundarapandiyan 2021 [4]	10	about +0.003–0.004 wt.%/build	more lack-of-fusion defects degrading high-cycle fatigue	fine-powder loss and more high-aspect-ratio particles
Borrelli 2024 [45]	multiple	oxygen up, hardness up	critical defect size larger	no significant fatigue difference

7. Remaining problems and outlook

Research on EB-PBF powder recovery and reuse has formed a fairly systematic body of knowledge, but the following problems remain.

(1) Scattered characterization approaches and the lack of unified criteria. The characterization dimensions are numerous (chemistry, morphology, particle size, rheology, charging), different instruments may even rank the flowability of the same powder oppositely, and no composite powder quality index is generally accepted. The EB-PBF suitability factor (ESF) of Shanbhag and Vlasea — a composite index of the relative changes of 13 indicators covering particle size, oxygen/nitrogen, flow and packing, which increases from 0.176 for virgin powder to 0.659 after 3 reuse cycles — and

DOI: 10.54254/2755-2721/2027.AD38964

the degradation assessment framework of Powell et al. are two representative attempts, but neither has been standardized [1, 61].

(2) Single-criterion reuse assessment. Most studies use oxygen content as the only criterion, whereas for IN718 the oxide inclusions and charging behavior may be more critical than oxygen content [8, 40], and for TiAl the Al loss and phase transformation are equally important [11]. Material-system-adaptive reuse criteria are a future direction.

(3) Insufficient online/in-situ monitoring. Powder quality assessment still relies mainly on offline sampling; the in-situ application of process logs [56] and ELO imaging [24] is just beginning, and integration with closed-loop process control and digital twins is still needed.

(4) Limited modeling and prediction capability. Oxidation kinetics modeling [36] and general degradation frameworks [25] have taken shape, but coupled models covering elemental evaporation, morphological evolution and rheological changes remain lacking.

(5) Limited closed-loop and life-cycle perspective. Research is mostly focused on the in-build loop; the regeneration of end-of-life powder (spatter, caked powder, over-limit powder), such as electron beam melting refining [51], and life-cycle assessment have received insufficient attention [61]. Mechanical recycling has also been explored: Richter et al. crushed support structures and heavily sintered residual powder into reclaimed powder, blended it with virgin powder and rebuilt parts; tensile and high/low-cycle fatigue tests showed that the reclaimed powder can partially replace virgin powder in structural integrity and fatigue performance [62]. The circular additive manufacturing framework of Chen et al. extends this to a larger material loop: scrap metal (retired components, machining chips, support waste) is converted by solid-state (mechanical crushing, hydrogenation–dehydrogenation) or melt-state (zone melting, electron beam refining, atomization remelting) recycling into regenerated spherical powder meeting AM requirements, closing the material–product–regenerated material loop; batch consistency, inclusion control and qualification of regenerated powder remain unsolved [17, 18].

Future research may proceed as follows: starting from the ESF, incorporating EB-PBF-specific degradation dimensions such as charging behavior and elemental evaporation losses, to build a unified powder quality evaluation and reuse criterion system applicable to different material systems [1, 7, 8, 11]; correlating ELO imaging signals with powder oxygen content/defect state, combined with process logs and machine learning to predict the powder state during raking [24]; developing multi-physics coupled degradation modeling; and promoting an integrated closed-loop system of feedstock–process–part–performance–recovery [6, 12, 25]. Chinese reviews have proposed similar directions, including improving the traceability of powder utilization, developing standardized blending strategies and standardizing the reuse flow [15, 16]; developing new AM-specific alloys with higher oxidation resistance and lower spattering tendency to extend powder cycle life at the source [17]; and quantitative cycle-coefficient management of cyclic powder use [55].

8. Conclusions

This paper systematically reviews and evaluates the important literature of the past fifteen years (2011–2026) on metal powder recovery and reuse in EB-PBF. The main conclusions are as follows.

(1) Powder recovery and recycling in EB-PBF is of significant economic importance: about 95%–98% of the un-melted powder can be recycled, but degradation during vacuum high-temperature building and recovery handling is unavoidable, involving oxidation, elemental evaporation, morphological damage, PSD drift and flowability deterioration, with pronounced material-system dependence.

DOI: 10.54254/2755-2721/2027.AD38964

(2) Oxygen pickup is the dominant degradation indicator for Ti-6Al-4V powder (Figure 2), the surface oxide film thickening with reuse from about 6.5 to about 7.5 nm (Figure 3); IN718 is dominated by surface Al-rich oxides and deteriorated charging behavior, while TiAl additionally suffers severe Al loss and phase transformation (Figure 4). Elemental evaporation (Al, Cr) occurs generally under vacuum at high temperature.

(3) Powder reuse slightly increases the strength and hardness of parts while decreasing ductility, impact toughness and high-cycle fatigue performance; fatigue is mediated mainly through lack-of-fusion defects, and surface roughness often outweighs powder degradation itself; HIP effectively restores fatigue performance, whereas oxide inclusions in IN718 are hard to eliminate.

(4) Fresh-powder blending (a 15%–30% fresh fraction is recommended), sieving management, process logs and ELO in-situ monitoring, and the ASTM standard series are the main quality-control means; the reuse limit (about 5–12 cycles by the oxygen limit; 21 cycles by acceptable static performance; Figure 8) is an engineering decision variable rather than a material constant.

(5) Current research still suffers from scattered characterization approaches, single-criterion reuse assessment and insufficient online monitoring; establishing standardized powder quality criteria and developing online monitoring and closed-loop recycling systems are the key directions for promoting green and efficient powder utilization in EB-PBF.

Declarations

Authorship: All contributions were made by Boxuan Wang: Conceptualization, Data curation, Formal analysis, Investigation, Methodology, Validation, Visualization, Writing – original draft, Writing – review & editing.

References

[1] Shanbhag, G., & Vlasea, M. (2021). Powder reuse cycles in electron beam powder bed fusion—variation of powder characteristics. *Materials, 14*(16), 4602. https://doi.org/10.3390/ma14164602

[2] Vock, S., Klöden, B., Kirchner, A., et al. (2019). Powders for powder bed fusion: A review. *Progress in Additive Manufacturing, 4*(4), 383–397. https://doi.org/10.1007/s40964-019-00078-6

[3] Popov, V. V., Katz-Demyanetz, A., Garkun, A., et al. (2018). The effect of powder recycling on the mechanical properties and microstructure of electron beam melted Ti-6Al-4V specimens. *Additive Manufacturing, 22*, 834–843. https://doi.org/10.1016/j.addma.2018.06.003

[4] Soundarapandiyan, G., Johnston, C., Khan, R. H. U., et al. (2021). The effects of powder reuse on the mechanical response of electron beam additively manufactured Ti6Al4V parts. *Additive Manufacturing, 46*, 102101. https://doi.org/10.1016/j.addma.2021.102101

[5] Popov, V. V., Lobanov, M. L., Stepanov, S. I., et al. (2021). Texturing and phase evolution in Ti-6Al-4V: Effect of electron beam melting process, powder re-using, and HIP treatment. *Materials, 14*(16), 4473. https://doi.org/10.3390/ma14164473

[6] Moghimian, P., Poirié, T., Habibnejad-Korayem, M., et al. (2021). Metal powders in additive manufacturing: A review on reusability and recyclability of common titanium, nickel and aluminum alloys. *Additive Manufacturing, 43*, 102017. https://doi.org/10.1016/j.addma.2021.102017

[7] Chiba, A., Daino, Y., Aoyagi, K., et al. (2021). Smoke suppression in electron beam melting of Inconel 718 alloy powder based on insulator–metal transition of surface oxide film by mechanical stimulation. *Materials, 14*(16), 4662. https://doi.org/10.3390/ma14164662

[8] Cordova, L., Raza, A., & Hryha, E. (2022). Rheological behavior of Inconel 718 powder for electron-beam melting. *Metals, 12*(7), 1231. https://doi.org/10.3390/met12071231

[9] Raza, A., & Hryha, E. (2021). Characterization of spatter and sublimation in Alloy 718 during electron beam melting. *Materials, 14*(20), 5953. https://doi.org/10.3390/ma14205953

[10] Sun, Y., Aindow, M., & Hebert, R. J. (2018). The effect of recycling on the oxygen distribution in Ti-6Al-4V powder for additive manufacturing. *Materials at High Temperatures, 35*(1-3), 217-224.

DOI: 10.54254/2755-2721/2027.AD38964

https://doi.org/10.1080/09603409.2017.1389133
[11] Wang, F., Song, M., Liang, Y., et al. (2025). Powder recycling for electron beam powder bed fusion of TiAl alloy. *Materials & Design, 257*, 114473. https://doi.org/10.1016/j.matdes.2025.114473
[12] Lopes, A. C., Pedroso, A. F. V., Silva, F. J. G., et al. (2026). Recyclability in metal additive manufacturing: Bridging powder lifecycle, defect evolution and fatigue-critical reliability across SLM and EBM. *Machines, 14*(7), 761. https://doi.org/10.3390/machines14070761
[13] Tang, H. P. (2020). Progress in engineering application research of Ti-6Al-4V alloy fabricated by powder bed electron beam 3D printing. *Materials China, 39*(7-8), 551-557. https://doi.org/10.7502/j.issn.1674-3962.202006031. (in Chinese)
[14] Liu, M., Guo, Y., Zhen, Z., et al. (2022). Research progress of Ti-6Al-4V alloy fabricated by selective electron beam melting. *Powder Metallurgy Industry, 32*(2), 84-89. https://doi.org/10.13228/j.boyuan.issn1006-6543.20210028. (in Chinese)
[15] Zhang, J. J., Li, B., Ren, H. T., et al. (2022). Research status of powder reuse in powder bed additive manufacturing. *Powder Metallurgy Technology*. https://doi.org/10.19591/j.cnki.cn11-1974/tf.2022070013. (in Chinese)
[16] Hu, J., Lyu, X. F., Shen, L. D., et al. (2022). Research progress on recycling and reuse of metal powder in powder bed fusion. *Powder Metallurgy Industry, 32*(3), 44-48. https://doi.org/10.13228/j.boyuan.issn1006-6543.20210035. (in Chinese)
[17] Pan, B., Han, L., Qiao, Y. F., et al. (2026). Research status on recycling and reuse of metal powder for powder bed fusion additive manufacturing. *Powder Metallurgy Industry, 36*(3), 149-157. https://doi.org/10.13228/j.boyuan.issn1006-6543.20250220. (in Chinese)
[18] Chen, X. Y., Tu, J. X., Lei, L. M., et al. (2026). Research status and prospects of circular additive manufacturing of metal material recovery. *Materials Reports*. (in Chinese)
[19] Jiao, M., Long, H., Xiao, B., et al. (2024). Electron beam powder bed fusion additive manufacturing: A comprehensive review and its development in China. *Additive Manufacturing Frontiers, 3*, 200177. https://doi.org/10.1016/j.amf.2024.200177
[20] Karlsson, J., Snis, A., Engqvist, H., et al. (2013). Characterization and comparison of materials produced by electron beam melting (EBM) of two different Ti-6Al-4V powder fractions. *Journal of Materials Processing Technology, 213*(12), 2109-2118. https://doi.org/10.1016/j.jmatprotec.2013.06.010
[21] Körner, C. (2016). Additive manufacturing of metallic components by selective electron beam melting—a review. *International Materials Reviews, 61*(5), 361-377. https://doi.org/10.1080/09506608.2016.1176289
[22] Tang, H. P., Qian, M., Liu, N., et al. (2015). Effect of powder reuse times on additive manufacturing of Ti-6Al-4V by selective electron beam melting. *JOM, 67*(3), 555-563. https://doi.org/10.1007/s11837-015-1300-4
[23] Petrovic, V., & Niñerola, R. (2015). Powder recyclability in electron beam melting for aeronautical use. *Aircraft Engineering and Aerospace Technology, 87*(2), 147-155. https://doi.org/10.1108/aeat-11-2013-0212
[24] Gardfjell, M., Reith, M., Franke, M., et al. (2023). In situ inclusion detection and material characterization in an electron beam powder bed fusion process using electron optical imaging. *Materials, 16*(12), 4220. https://doi.org/10.3390/ma16124220
[25] Hryha, E. (2025). Powder for metal additive manufacturing: Production, reuse and recycling. *Journal of the Japan Society of Powder and Powder Metallurgy, 72*(Suppl.), S83-S90. https://doi.org/10.2497/jjspm.14b-t6-03
[26] Ren, P., Ouyang, Y., Mu, J., et al. (2025). Metal powder atomization preparation, modification, and reuse for additive manufacturing: A review. *Progress in Materials Science, 152*, 101449. https://doi.org/10.1016/j.pmatsci.2025.101449
[27] Li, J., Liu, W., Shen, J., et al. (2024). Research progress of the metal powder reuse for powder bed fusion additive manufacturing technology. *Powder Technology, 441*, 119815. https://doi.org/10.1016/j.powtec.2024.119815
[28] Lanzutti, A., & Marin, E. (2024). The challenges and advances in recycling/re-using powder for metal 3D printing: A comprehensive review. *Metals, 14*(8), 886. https://doi.org/10.3390/met14080886
[29] Cao, Y., Delin, M., Kullenberg, F., et al. (2020). Surface modification of Ti-6Al-4V powder during recycling in EBM process. *Surface and Interface Analysis, 52*(12), 1066-1070. https://doi.org/10.1002/sia.6847
[30] Gruber, H., Henriksson, M., Hryha, E., et al. (2019). Effect of powder recycling in electron beam melting on the surface chemistry of Alloy 718 powder. *Metallurgical and Materials Transactions A, 50*(9), 4410-4422. https://doi.org/10.1007/s11661-019-05333-7
[31] ASTM International. (2021). F2924-14(2021), Standard specification for additive manufacturing titanium-6 aluminum-4 vanadium with powder bed fusion. West Conshohocken, PA: ASTM International.
[32] Nandwana, P., Peter, W. H., Dehoff, R. R., et al. (2016). Recyclability study on Inconel 718 and Ti-6Al-4V powders for use in electron beam melting. *Metallurgical and Materials Transactions B, 47*(1), 754-762.

DOI: 10.54254/2755-2721/2027.AD38964

https://doi.org/10.1007/s11663-015-0477-9
[33] Ghods, S., Schultz, E., Wisdom, C., et al. (2020). Electron beam additive manufacturing of Ti6Al4V: Evolution of powder morphology and part microstructure with powder reuse. *Materialia, 9*, 100631. https://doi.org/10.1016/j.mtla.2020.100631
[34] Derimow, N., & Hrabe, N. (2021). Oxidation in reused powder-bed fusion additive manufacturing Ti-6Al-4V feedstock: A brief review. *JOM, 73*(11), 3618-3638. https://doi.org/10.1007/s11837-021-04872-y
[35] Schwerdtfeger, J., & Körner, C. (2014). Selective electron beam melting of Ti–48Al–2Nb–2Cr: Microstructure and aluminium loss. *Intermetallics, 49*, 29-35. https://doi.org/10.1016/j.intermet.2014.01.004
[36] Siblani, M., Ollivier, M., Chartrand, P., et al. (2025). Modeling the oxidation kinetics of Ti-6Al-4V spherical powder at high temperatures. *High Temperature Corrosion of Materials, 102*(4), 18. https://doi.org/10.1007/s11085-025-10336-4
[37] Chandroth, A. M., Giraldo-Osorno, P. M., Nyborg, L., et al. (2024). The effect of powder reuse on electron beam melting for biomedical implants. *Materials, 17*(19), 4701. https://doi.org/10.3390/ma17194701
[38] Zhong, B., Liu, X. Y., Wu, W., et al. (2020). Study on powder characteristics of Ti-6Al-4V alloy recycled by electron beam 3D printing. *Titanium Industry Progress, 37*(2), 39-42. https://doi.org/10.13567/j.cnki.issn1009-9964.2020.02.011. (in Chinese)
[39] Ghods, S., Schur, R., Schultz, E., et al. (2021). Powder reuse and its contribution to porosity in additive manufacturing of Ti6Al4V. *Materialia, 15*, 100992. https://doi.org/10.1016/j.mtla.2020.100992
[40] Gruber, H., Luchian, C., Hryha, E., et al. (2020). Effect of powder recycling on defect formation in electron beam melted Alloy 718. *Metallurgical and Materials Transactions A, 51*(5), 2430-2443. https://doi.org/10.1007/s11661-020-05674-8
[41] Montelione, A., Ghods, S., Schur, R., et al. (2020). Powder reuse in electron beam melting additive manufacturing of Ti6Al4V: Particle microstructure, oxygen content and mechanical properties. *Additive Manufacturing, 35*, 101216. https://doi.org/10.1016/j.addma.2020.101216
[42] Schur, R., Ghods, S., Wisdom, C., et al. (2021). Mechanical anisotropy and its evolution with powder reuse in electron beam melting AM of Ti6Al4V. *Materials & Design, 200*, 109450. https://doi.org/10.1016/j.matdes.2021.109450
[43] Wanjara, P., Backman, D., Sikan, F., et al. (2022). Microstructure and mechanical properties of Ti-6Al-4V additively manufactured by electron beam melting with 3D part nesting and powder reuse influences. *Journal of Manufacturing and Materials Processing, 6*(1), 21. https://doi.org/10.3390/jmmp6010021
[44] Grell, W. A., Solis-Ramos, E., Clark, E., et al. (2017). Effect of powder oxidation on the impact toughness of electron beam melting Ti-6Al-4V. *Additive Manufacturing, 17*, 123–134. https://doi.org/10.1016/j.addma.2017.08.002
[45] Borrelli, R., Bellini, C., Berto, F., et al. (2024). The impact of Ti6Al4V powder reuse on the quality of electron beam powder bed fusion parts. *Progress in Additive Manufacturing, 9*(5), 1475–1490. https://doi.org/10.1007/s40964-023-00560-2
[46] Schur, R., Ghods, S., Schultz, E., et al. (2020). A fractographic analysis of additively manufactured Ti6Al4V by electron beam melting: Effects of powder reuse. *Journal of Failure Analysis and Prevention, 20*(3), 794–803. https://doi.org/10.1007/s11668-020-00875-0
[47] Bellini, C., Borrelli, R., Di Cocco, V., et al. (2024). Fatigue crack growth in Ti-6Al-4V EBMed samples: Impact of powder recycling. *Procedia Structural Integrity, 53*, 129–135. https://doi.org/10.1016/j.prostr.2024.01.016
[48] Wang, P., Nai, M. L. S., Ng, F. L., et al. (2022). Revealing mechanisms underlying powder reusability of Ti-48Al-2Cr-2Nb intermetallic in electron beam powder bed fusion process. *Additive Manufacturing, 59*, 103155. https://doi.org/10.1016/j.addma.2022.103155
[49] Yang, X., Sun, C., Wang, F., et al. (2023). Effect of reuse times on H13 powder properties processed by selective electron beam melting. *Powder Metallurgy, 66*(2), 107–115. https://doi.org/10.1080/00325899.2022.2115758
[50] Vutova, K., Stefanova, V., Vassileva, V., et al. (2022). Recycling of technogenic CoCrMo alloy by electron beam melting. *Materials, 15*(12), 4168. https://doi.org/10.3390/ma15124168
[51] Vutova, K., Stefanova, V., Markov, M., et al. (2023). Study on hardness of heat-treated CoCrMo alloy recycled by electron beam melting. *Materials, 16*(7), 2634. https://doi.org/10.3390/ma16072634
[52] Gu, Y., Yuan, H., Song, Z., et al. (2026). Microscopic characterization of oxygen content accumulation and powder recyclability in selective electron beam melting of copper. *Frontiers in Materials, 13*, 1789314. https://doi.org/10.3389/fmats.2026.1789314
[53] Guschlbauer, R., Burkhardt, A. K., Fu, Z., et al. (2020). Effect of the oxygen content of pure copper powder on selective electron beam melting. *Materials Science and Engineering: A, 779*, 139106. https://doi.org/10.1016/j.msea.2020.139106

DOI: 10.54254/2755-2721/2027.AD38964

[54] Blasco Puchades, J. R., Portolés Griñán, L., Bloem Irazabal, C. A., et al. (2026). Reuse of pure copper in electron beam powder bed fusion. *The International Journal of Advanced Manufacturing Technology*. https://doi.org/10.1007/s00170-025-17180-5

[55] Hu, J. W., Li, Z. L., Peng, W., et al. (2025). Cyclic use of TC4 powder in selective laser melting. *Powder Metallurgy Industry, 35*(2), 81-90. https://doi.org/10.13228/j.boyuan.issn1006-6543.20230191. (in Chinese)

[56] Chandrasekar, S., Coble, J. B., Yoder, S., et al. (2020). Investigating the effect of metal powder recycling in electron beam powder bed fusion using process log data. *Additive Manufacturing, 32*, 100994. https://doi.org/10.1016/j.addma.2019.100994

[57] ASTM International. (2021). F3049-14(2021), Standard guide for characterizing properties of metal powders used for additive manufacturing processes. West Conshohocken, PA: ASTM International.

[58] ASTM International. (2018). F3302-18, Standard for additive manufacturing — finished part properties — standard specification for titanium alloys via powder bed fusion. West Conshohocken, PA: ASTM International.

[59] Standards Press of China. (2017). GB/T 34508-2017, Powder bed electron beam additive manufacturing TC4 alloy material. Standards Press of China. Beijing.

[60] Standards Press of China. (2024). GB/T 44194-2024, Additive manufacturing — Technical specification for reuse of metal powders. Standards Press of China. Beijing.

[61] Powell, D., Rennie, A. E. W., Geekie, L., et al. (2020). Understanding powder degradation in metal additive manufacturing to allow the upcycling of recycled powders. *Journal of Cleaner Production, 268*, 122077. https://doi.org/10.1016/j.jclepro.2020.122077

[62] Richter, J., Wegener, T., Kratzsch, R., et al. (2023). On the structural integrity and fatigue performance of additively manufactured Ti-6Al-4V parts processed using mechanically recycled powders. *International Journal of Fatigue, 176*, 107903. https://doi.org/10.1016/j.ijfatigue.2023.107903